MEDWIN PUBLISHERS
Committed to Create Value for Researchers

Journal of Orthopedics & Bone Disorders
ISSN: 2577-297X

Spinal Segment Model and its 3D Printing

Sergeev AN, Yuriev Yu V and Pichkhidze Ya S*

Yuri Gagarin State Technical University of Saratov, Saratov, Russian Federation

***Corresponding author:** Pichkhidze Sergey Ya, Yuri Gagarin State Technical University of Saratov, Saratov, Russian Federation

Research Article

Volume 10 Issue 4

Received Date: August 07, 2026

Published Date: November 26, 2026

DOI: 10.23880/jobd-16000304

Abstract

Spinal diseases are widespread, and surgical intervention with the installation of implants is often required to restore spinal function. Modern technologies, such as computer modeling and 3D printing, make it possible to create personalized constructs optimized for biomechanical characteristics and biocompatibility. The aim of the study was to develop a personalized interbody mesh spinal implant, to carry out its biomechanical analysis using the finite element method, and to verify manufacturability by 3D printing a physical mock-up of the spinal segment from polyetheretherketone (PEEK). Materials and Methods. Based on X-ray images of the thoracic spine (Th9–Th11), processed in RadiAnt DICOM Viewer software with contrast correction, a computer model of a PEEK mesh implant was developed in SolidWorks 2024 using the Simulation module. Von Mises stress calculations and safety factor analysis were performed for loads from 200 to 700 N. Based on the virtual model, a 3D-printed physical mock-up of the "vertebra – implant – vertebra" system was produced from PEEK. Results. A computer model of an implant integrated into a spinal segment was built. The results of finite element analysis showed that the construct maintains integrity and has a sufficient safety factor in the load range of 200–700 N, corresponding to physiological conditions. Visualization of stress diagrams and damage percentages confirmed the reliability of the design. Conclusion. The combined use of computer modeling and 3D printing technologies makes it possible to create personalized spinal implants with predictable mechanical properties. This approach helps to reduce surgical risks and can be used for preoperative planning and the manufacture of biocompatible constructs © PNRPU.

Keywords: 3D Printing; Spine; Implant; Computer Modeling; Biomechanics; Finite Element Analysis; Safety Factor

Introduction

The spine, being the central axial organ of the musculoskeletal system, performs critically important functions including support, movement, and protection of the spinal cord. Degenerative-dystrophic diseases, injuries, and oncological lesions of the spinal column remain among the most widespread and socially significant problems in contemporary orthopedics and neurosurgery [1-24]. Traditional conservative treatment methods are often ineffective in pronounced structural disorders, which necessitates surgical interventions aimed at stabilizing and restoring the anatomical integrity of the damaged segment [4,11].

One of the key directions in spinal surgery is endoprosthetics the replacement of a damaged intervertebral disc or vertebral body with an artificial implant. Despite significant progress in bioengineering and materials science, serious challenges remain regarding the long-term stability and functionality of implants. These include the risk of construct instability, stress-shielding phenomena leading to resorption of adjacent bone tissue, and aseptic loosening [2,3,21]. These complications are largely caused by a mismatch between the mechanical characteristics of the implant and the properties of natural bone and the patient's individual anatomical features [23-31].

CC BY

In this context, personalization of the endoprosthesis development approach is not merely promising but necessary. Standardized mass-produced implants cannot fully account for unique variations in the dimensions, shape, and tilt angles of vertebrae in each individual patient. The solution to this problem lies in the application of advanced digital technologies forming a closed-loop cycle from diagnosis to device fabrication [6,8,26].

The first and fundamental stage of this cycle is accurate preoperative diagnosis and planning. Modern imaging methods such as radiography and computed tomography provide the necessary data [10]. However, quantitative characterization and construction of an accurate 3D model often require image post-processing, including contrast adjustment, which enables clear differentiation of bone structures from surrounding tissues [5,30].

Based on this data, it becomes possible to create a digital model of the future implant using computer-aided design (CAD) systems. However, geometric correspondence is only part of the task. Critically important is the prediction of implant behavior under real mechanical loads. This is where finite element analysis (FEA) methods come in, enabling virtual testing of the construct for strength, stiffness, and fatigue life by simulating various physiological and peak loads [15,16,18,20,28,32-34]. This allows the engineer to optimize implant design, including its internal structure (e.g., porous mesh), to achieve mechanical properties as close as possible to bone tissue, thereby minimizing the risk of biomechanical complications [9,13,22].

The final stage, linking the virtual design to real practice, is additive manufacturing (3D printing). This technology enables the fabrication of both a functional prototype for preoperative evaluation and fitting, and a finished product from bioinert or bioresorbable materials [16,17,33]. Using 3D printing to create mock-ups from thermoplastics (e.g., PEEK) provides the surgeon with a unique opportunity for tactile study of anatomy and surgical planning on a physical, rather than purely virtual, model [16,25].

In recent years (2020–2025), several research groups have reported on the use of additively manufactured PEEK interbody implants in vertebral surgery: advantages of porous and mesh architectures have been demonstrated in terms of reducing stress shielding and promoting osseointegration, as well as the possibility of individual adaptation of geometry to patient anatomy [35-42]. However, in the domestic literature, studies combining in a single closed loop the acquisition of initial radiological data, CAD modeling of a mesh PEEK construct, finite element analysis, and additive fabrication of a physical mock-up are limited. The novelty of the present work consists precisely in the implementation of such a closed-loop cycle using standard available software tools (RadiAnt DICOM Viewer, SolidWorks with the Simulation module) and standard FDM equipment for PEEK printing, making the proposed methodology reproducible in an ordinary engineering and medical laboratory. Thus, the integrated application of medical imaging, computer modeling, and 3D printing technologies forms a new approach in spinal surgery [6,26,32]. The aim of the present study was to develop and perform a comprehensive biomechanical analysis of a spinal segment with an implant created using the described technological cycle, followed by experimental verification through 3D-printed fabrication of a physical mock-up.

Model Construction

Radiographic Analysis and Geometric Model Construction

The object of study was the lower thoracic vertebrae (Th9, Th10, Th11). This segment was selected because the transitional zone of the lower thoracic spine experiences significant axial loads and is one of the most common sites for traumatic and degenerative-dystrophic lesions requiring interbody fusion [28]. X-ray images in two projections (posterior and lateral views) were obtained and processed in RadiAnt DICOM Viewer software. To improve visualization and measurement accuracy of vertebral parameters, the contrast correction function with the preset “CT Bone” profile was used (Figures 1 & 2).

Contrast adjustment enables better examination of the obtained radiographic image. The program’s toolset also allows measurement of vertebral dimensions for constructing the future computer model. Based on radiographic analysis data, a computer model of the implant integrated into the vertebral segment of the thoracic spine was developed, comprising the Th9 – vertebra – Th11 segment (Figure 3) [7,10]. The implant represents a hollow cylindrical mesh spacer with the following geometric parameters: outer diameter – 25 mm, inner diameter – 23 mm, height – 25 mm, strut thickness – 1 mm, mesh pore size – approximately 2 mm, estimated porosity – approximately 60%. The choice of a cylindrical hollow form with through-perforations was dictated by the need to ensure, on one hand, sufficient contact area with the vertebral endplates (reducing the risk of implant subsidence compared to small-support constructs), and on the other – to create channels for bone tissue ingrowth through the implant body. The biomechanical system also includes a transpedicular fixation system (TPF), providing stabilization of the spinal motion segment; the geometry of the TPF elements was based on standard dimensions of applied constructs. Using the built-in program tools, it is possible to measure the thickness and height of the studied

Copyright© Pichkhidze Ya S, et al.

vertebrae: Th9 – 3.21 cm, 2.41 cm; Th10 – 3.26 cm, 2.52 cm; Th11 – 3.34 cm, 2.54 cm (thickness and height, respectively).

These parameters will determine the dimensions of the 3D model of the implant.

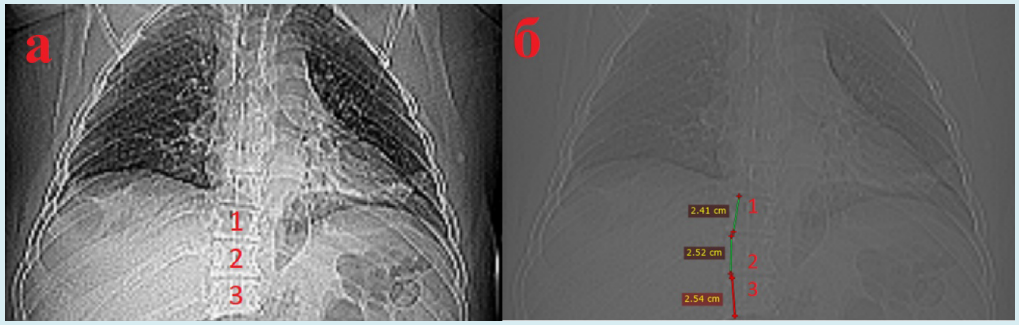

Figure 1: Chest X-ray (posterior view): 1 – Th9 vertebra; 2 – Th10 vertebra; 3 – Th11 vertebra (a – before contrast adjustment; b – after contrast adjustment).

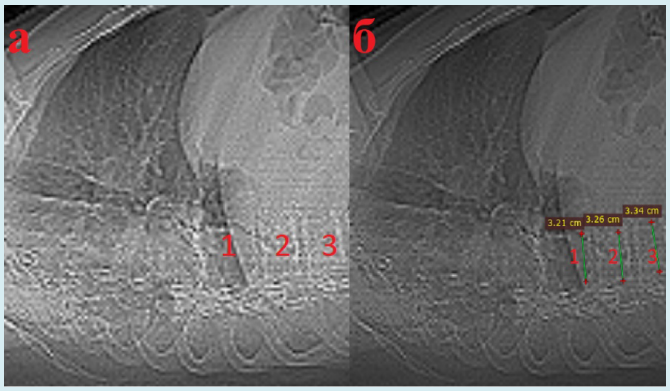

Figure 2: Chest X-ray (lateral view): 1 – Th9 vertebra; 2 – Th10 vertebra; 3 – Th11 vertebra (a – before contrast adjustment; b – after contrast adjustment).

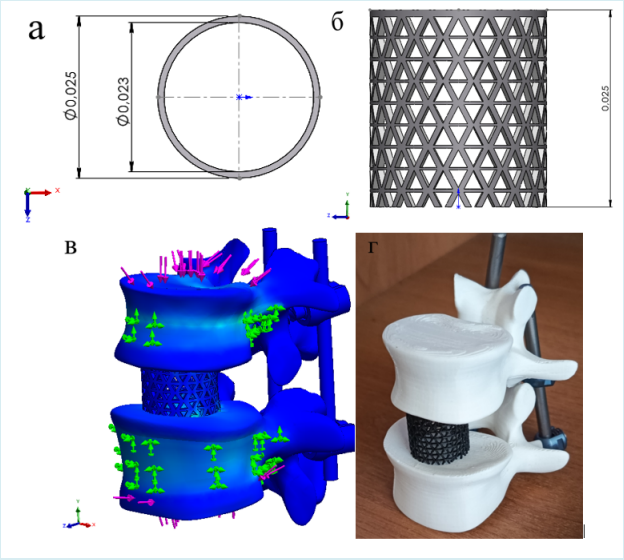

Figure 3: Computer model: a – implant (top view); b – implant (side view); c – system Th9 vertebra – implant – Th11 vertebra with loading and fixation lines; d – 3D-printed system model.

Copyright© Pichkhidze Ya S, et al.

3D Printing of the Mock-up

3D printing of the "vertebra – implant – vertebra" system mock-up was carried out using fused deposition modeling (FDM). A PEEK filament with a diameter of 1.75 mm was used as the implant material. Model preparation for printing (slicing) was performed in specialized slicer software with subsequent export of G-code to a printer equipped with a high-temperature extruder and a heated bed/enclosed chamber, which is necessary for correct processing of PEEK. The implant was printed with 100% infill and a vertical orientation of the cylinder axis along the Z-axis to ensure maximum strength in the direction of operational load. Vertebral templates used for tactile and anatomical assessment of the construct were made from standard PLA or ABS plastic.

Study of the Model

Input Data

For conducting the finite element calculation and evaluating the fatigue life of the "vertebra – implant – vertebra" segment, the initial data on the mechanical properties of the implant material – PEEK – were entered into the Simulation module (SolidWorks). Material characteristics were specified from the program's material library and subsequently used in calculating von Mises equivalent stresses, safety factor, and fatigue damage of the construct. The accepted values of elastic, strength, and physical characteristics of PEEK are given in Table 1.

Property	Value	Unit
Elastic modulus	3900	N/mm^2
Poisson's ratio	0.4	–
Shear modulus	318.9	N/mm^2
Mass density	1310	kg/m^3
Ultimate tensile strength	95	N/mm^2
Compressive strength	125	N/mm^2
Yield strength	110	N/mm^2

Table 1: Mechanical properties of the implant material (PEEK).

PEEK belongs to the class of thermoplastic polymers, which are characterized by the absence of a clearly defined physical endurance limit. Therefore, when assessing the fatigue life of the implant, a monotonically decreasing fatigue curve (S–N curve, Wöhler curve) was defined, establishing the relationship between the alternating stress amplitude S and the number of cycles to failure N.

The S–N curve was formed for a cycle asymmetry ratio R = –1, corresponding to fully reversed (alternating) loading with zero mean stress. Interpolation of intermediate values between nodal points was performed using a double logarithmic (log-log) scheme, applied due to the large values of N. The nodal points of the curve cover the range from 100 to 1,000,000 loading cycles, corresponding to the high-cycle fatigue region. The form of the specified fatigue curve is shown in Figure 4.

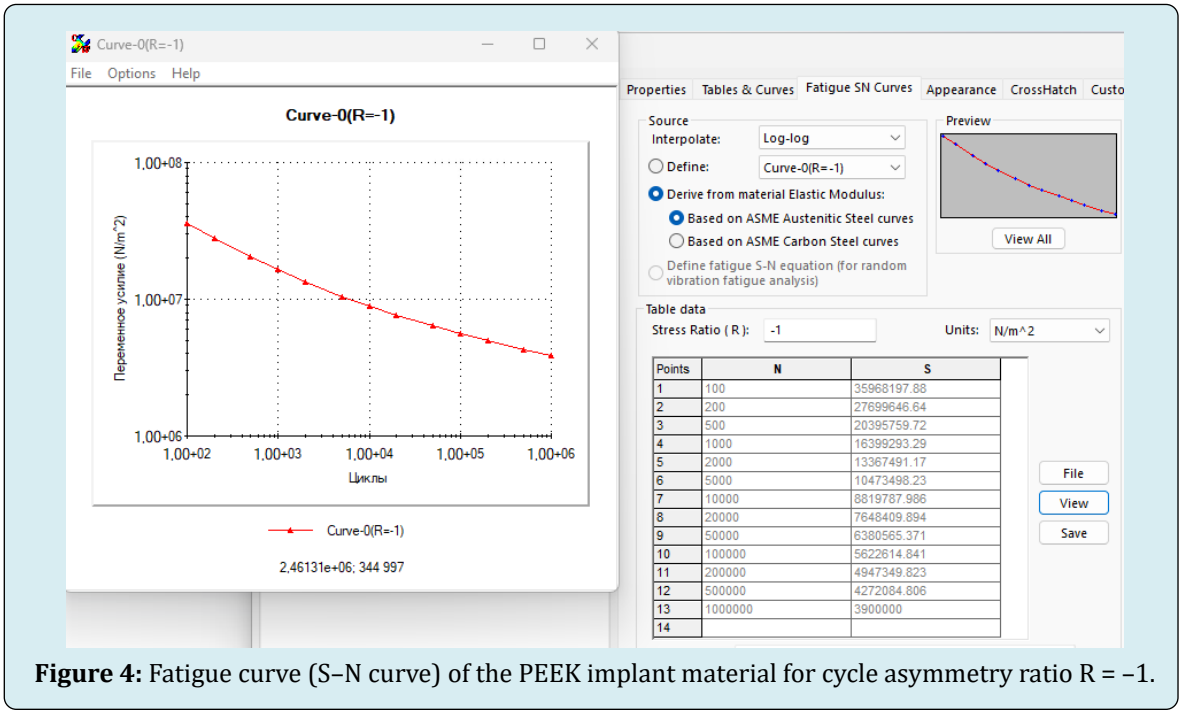

Figure 4: Fatigue curve (S–N curve) of the PEEK implant material for cycle asymmetry ratio R = –1.

Copyright© Pichkhidze Ya S, et al.

Finite Element Analysis

To assess the mechanical reliability of the construct, a finite element analysis was performed in the Simulation module (SolidWorks). The "vertebra – implant – vertebra" system model was fixed with a rigid constraint (all degrees of freedom of the lower face nodes were fixed); a uniformly distributed compressive load in the range of 200 to 700 N was applied to the upper face of the Th9 vertebra and the lower face of the Th11 vertebra, corresponding to conditions of primary stabilization of the construct and physiological loads on the thoracic spine [12,19,27,29]. The contact between the implant and vertebrae was set as "bonded," corresponding to the immediately post-implantation state. The following material mechanical characteristics were used in the calculation: for cortical bone tissue of the vertebrae – Young's modulus E = 12 GPa, Poisson's ratio ν = 0.3; for the implant material (PEEK) – E = 3.9 GPa, ν = 0.4. The finite element mesh was built using second-order tetrahedral elements (Solid186); the maximum element size was 1.5 mm in the contact zone and 3 mm in other areas; the total number of nodes exceeded 80,000. Solution convergence was confirmed by a 30% reduction in element size without significant change in peak stress values. The program performs calculation using the von Mises formula (1), used to evaluate equivalent stress [13]:

$$\sigma_{vonimes} = \sqrt{\frac{(\sigma_1 - \sigma_2)^2 + (\sigma_2 - \sigma_3)^2 + (\sigma_1 - \sigma_3)^2}{2}} \quad (1)$$

where: σ_1, σ_2, σ_3 – principal stresses.

The safety factor (Factor of Safety, FOS) was used as an additional integral criterion showing how many times the ultimate material strength exceeds the calculated equivalent stress in the most loaded zone of the construct. For a mesh implant, this indicator is particularly important since local stress concentrations may occur in strut elements and in areas of contact with vertebral endplates.

In SolidWorks Simulation, after completing the static calculation, the program generates a FOS map for the finite element mesh nodes and elements. When using the von Mises maximum stress criterion, the equivalent stress at each calculation point is compared with the limiting stress of the material specified in the material properties (equation 2). In the present calculation, the ultimate strength σu = 100 MPa was adopted as the limiting value for PEEK.

$$FOS_i = \frac{\sigma_{add}}{\sigma_{vonimes}}; \; FOS_{\min} = \min(FOS_i) \quad (2)$$

If FOS is greater than 1, the calculated stress is below the allowable level and the construct is sufficiently reliable; when FOS equals 1, the limiting state is reached; when FOS is less than 1, strength failure is possible. Therefore, in interpreting the SolidWorks diagram, the determining factor is the minimum safety factor corresponding to the most loaded region of the model. The color scale on the diagram shows the safety distribution across the construct: minimum values indicate potentially critical zones, while very large values typically refer to lightly loaded areas and are not determining from a calculation standpoint.

In the calculations performed, the minimum FOS values at loads of 200, 300, 500, and 700 N were 14, 9.5, 5.7, and 4.1, respectively, all greater than unity, indicating preservation of the safety factor in the investigated load range.

Fatigue Strength Calculation

Static finite element analysis characterizes the behavior of the construct under a single application of maximum load, but does not enable prediction of failure developing as a result of repeated cyclic loading. Under real operating conditions, the interbody implant is subjected not to static but to alternating load: during walking, bending, and rotation of the trunk, the spinal motion segment experiences repeated loading and unloading cycles. Over the calculated service life, the number of such cycles reaches 10^6–10^8, with material failure potentially occurring at stresses significantly below the ultimate strength. This phenomenon, called material fatigue, is one of the main causes of failure in load-bearing constructs, including orthopedic implants [13]. In this regard, in addition to the static calculation, an assessment of the fatigue strength (durability) of the mesh PEEK implant was performed in the Simulation module.

The fatigue life calculation was performed based on a fatigue study, which used the results of the previously conducted static analysis of the "vertebra – implant – vertebra" system as input data. Since physiological loading of the spine is pulsating in nature – the load is applied and removed without changing sign – the fatigue event was defined as a constant amplitude event with cycle asymmetry ratio R = σmin/σmax = 0 (zero-based cycle). The number of loading cycles was taken in the high-cycle fatigue range (~1 million cycles), consistent with the practice adopted in standard resource tests for interbody implants.

At each point of the finite element mesh, the alternating (amplitude) stress of the cycle σ_a and the mean stress of the cycle σ_m are determined by equations (3) and (4):

$$\sigma_a = \frac{\sigma_{\max} - \sigma_{\min}}{2} \quad (3)$$

$$\sigma_m = \frac{\sigma_{\max} - \sigma_{\min}}{2} \quad (4)$$

where σmax and σmin are the maximum and minimum stresses of the cycle, respectively. The von Mises equivalent stress, consistent with the static calculation of the construct, was used as the calculation stress component for determining

Copyright© Pichkhidze Ya S, et al.

the number of cycles to failure.

The relationship between the cyclic stress amplitude S and the number of cycles to failure N was set by the fatigue curve of the implant material (S–N curve, or Wöhler curve). For thermoplastics, to which PEEK belongs, a clearly defined endurance limit (horizontal portion of the S–N curve) is absent; therefore, a monotonically decreasing curve was used, constructed from experimental fatigue test data [35]. Interpolation of intermediate values between nodal points of the curve was performed using a double logarithmic (log-log) scheme applied due to the large values of N.

Fatigue curves are generally obtained for fully reversed loading (R = −1, zero mean stress), whereas in the problem under consideration the mean stress of the cycle is non-zero. To account for the effect of non-zero mean stress, the Goodman correction was applied, according to which the equivalent alternating stress reduced to zero mean σar is determined by the expression:

$$\sigma_{ar} = \sigma_a \left(\frac{1-\sigma_m}{\sigma_u}\right) \quad (5)$$

where σu is the ultimate strength of the material (for PEEK, σu = 100 MPa is adopted). The Goodman method was chosen as the most conservative for polymer materials, providing a durability assessment with a safety margin.

Accumulation of fatigue damage under load was described by the linear damage summation rule (Palmgren–Miner rule):

$$D = \sum \frac{n_i}{Ni} \quad (6)$$

where n_i is the number of cycles completed at the i-th alternating stress level; N_i is the number of cycles to failure at the same stress level, determined from the S–N curve. Fatigue failure is predicted when the cumulative damage reaches D = 1 (100%).

Based on the calculation results, the Simulation module generates diagrams: a Damage diagram showing the percentage of exhausted fatigue life; and a Load Factor diagram showing by how many times the applied load amplitude can be increased before reaching the limiting fatigue state.

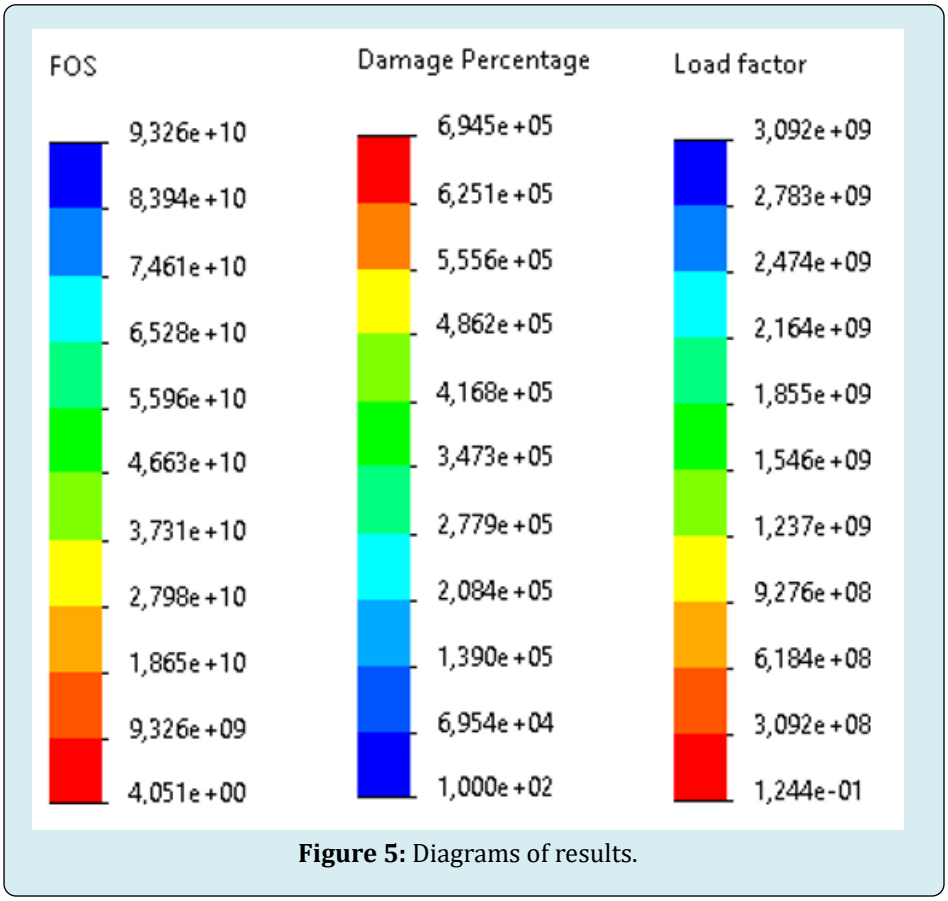

Figure 5: Diagrams of results.

Copyright© Pichkhidze Ya S, et al.

The fatigue life calculation was performed for the same load range of 200–700 N as the static analysis. It was established that the minimum predicted implant durability was 950,560 cycles, and the maximum fatigue damage over 1,000,000 loading cycles did not exceed 694,500%, corresponding to a load factor of 0.124. The zones of minimum durability are localized in the area of contact between the implant and the vertebrae, coinciding with the stress concentration zones identified in the static calculation. The Load Factor and damage diagrams are shown in Fig. 5. The obtained values confirm that in the investigated range of physiological loads, the construct maintains fatigue strength throughout the calculated service life.

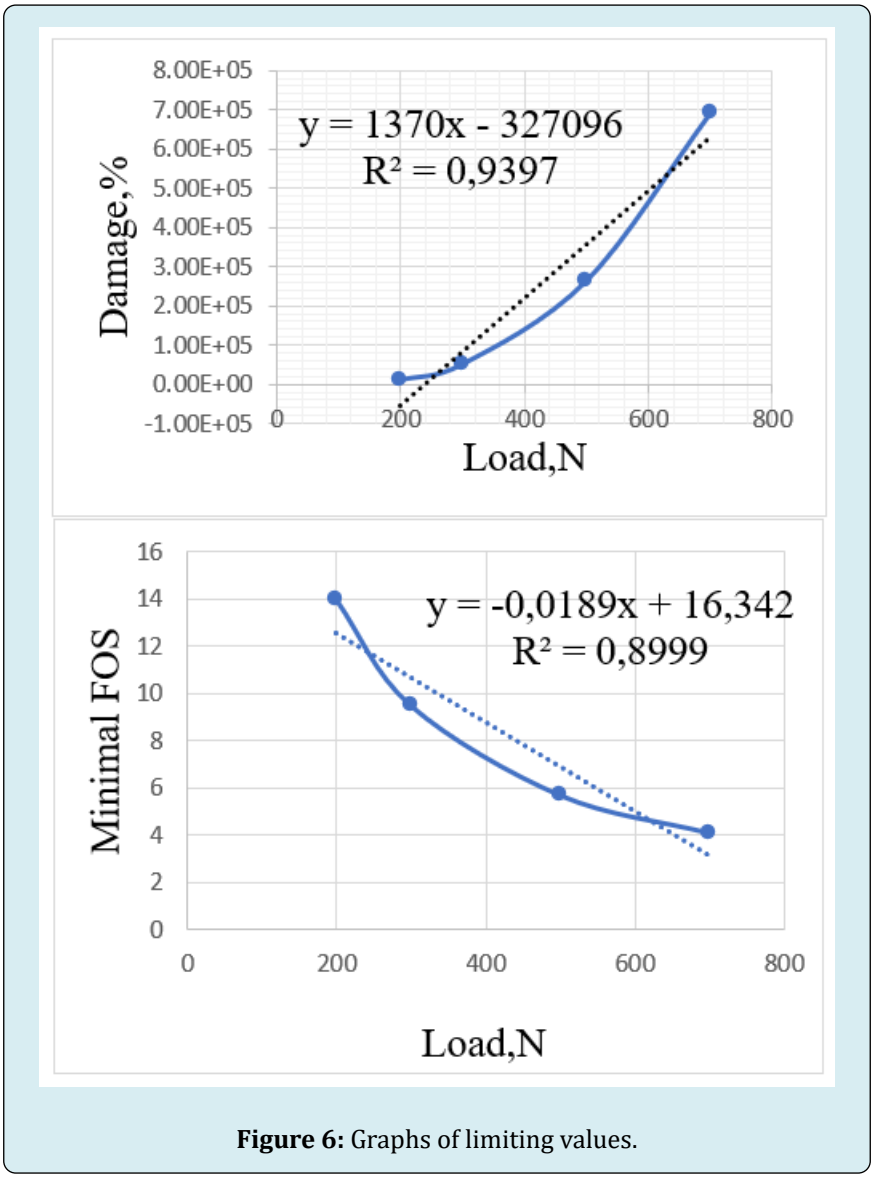

Figure 6: Graphs of limiting values.

Results

The calculation results, showing the change in the percentage of damage as a function of the applied loads, are presented in Fig. 6. A relationship can be traced between the load level and the degree of implant damage, enabling conclusions about the reliability of the construct under various load scenarios.

The work performed ensured the creation of a reliable computer model of a mesh implant for interbody spinal fusion and its comprehensive verification of mechanical stability. This constitutes an important stage toward the introduction of such implants into medical practice, as it allows ensuring their safety and effectiveness in clinical conditions [43,44].

Copyright© Pichkhidze Ya S, et al.

Discussion

The obtained finite element analysis results are comparable with data from analogous studies on the biomechanics of spinal implants. In particular, safety factor values in the range of 4.1–14.0 at loads of 200–700 N are consistent with results from studies on mesh PEEK spacers published in the international literature [34]. This indicates the correctness of the adopted assumptions and the calculation methodology used.

Among the advantages of the proposed approach, the following should be noted: a closed "diagnosis – modeling – verification" cycle; use of publicly available software (RadiAnt, SolidWorks); the possibility of fabricating preoperative mock-ups from PEEK without additional equipment.

At the same time, limitations of the present study must be noted. First, vertebral geometry was constructed based on two-projection radiography rather than computed tomography, which reduces the accuracy of reproducing the three-dimensional anatomy of the vertebral endplates. Second, the adopted "bonded" contact model does not account for possible micromotion at the bone-implant interface, which may lead to overestimation of the calculated safety factor compared to real in vivo conditions. Third, the calculation was performed only for axial compression without considering bending and torsional moments arising during trunk inclination and rotation. Physical verification of the simulation on the fabricated specimen (mechanical compression/torsion tests) is planned as part of subsequent stages of the work.

Conclusion

An algorithm for creating a personalized spinal segment has been developed, comprising the following stages: acquisition and processing of radiographic images, computer model construction, finite element analysis, and 3D printing of the physical mock-up.

The results of biomechanical modeling confirmed sufficient strength and reliability of the developed mesh implant construct in the physiological load range (200–700 N).

The use of 3D printing technology enables the creation of an accurate physical mock-up of the spinal segment that can be used for preoperative planning, implant fitting, and training.

Prospects for the work are related to conducting mechanical tests on the fabricated specimen to verify computer modeling results, expanding load scenarios (bending, torsion), transitioning to geometry construction based on computed tomography data, as well as studies of biocompatible materials and preclinical testing of the developed methodology.

Conflict of Interest

The authors declare no conflict of interest.

References

1. Amirdzhanova VN, Goryachev DV, Korshunov NI, Rebrov AP, Sorotskaya VN (2008) Population quality of life indicators according to the SF-36 questionnaire (results of the multicenter MIRAZH quality of life study). Nauchno-Prakticheskaya Revmatologiya 1: 36-48.

2. Baikov ES, Baikalov AA (2017) Relationship between biomechanical and biochemical parameters of spinal motion segments and recurrence of lumbar intervertebral disc herniations. Khirurgiya Pozvonochnika 4: 61-68.

3. Barabash Yu A, Ivanov DV, Bogatov VB, Lychagin AV (2021) Biomechanical approach to selecting the type of intramedullary fixator for a simulated femoral fracture. Russian Journal of Biomechanics 25(2): 209-217.

4. Berdyugin KA, Chertkov AK, Shtadler DI, Berdyugina OV (2010) On unsatisfactory outcomes of transpedicular spinal fixation. Khirurgiya Pozvonochnika 7(4): 19-24.

5. Beskrovny AS, Bessonov LV, Ivanov DV, Kirillova IV, Kossovich L Yu (2020) Using a convolutional neural network to automate construction of two-dimensional solid models of vertebrae. Izvestiya Saratovskogo Universiteta. New Series. Mathematics. Mechanics. Informatics 20(4): 502-516.

6. Beskrovny AS, Bessonov LV, Golyadkina AA, Dol AV, Ivanov DV, et al. (2021) Development of a clinical decision support system in traumatology and orthopedics. Biomechanics as a preoperative planning tool. Russian Journal of Biomechanics 25(2): 118-133.

7. Beskrovny AS, Bessonov LV, Ivanov DV, Zolotov VS, Sidorenko DA, et al. (2021) Construction of three-dimensional solid models of vertebrae using convolutional neural networks. Izvestiya Saratovskogo Universiteta. New Series. Mathematics. Mechanics. Informatics 21(3): 368-378.

8. Bessonov LV, Veliev VM, Ivanov DV, Zolotov VS, Dmitriev PO, et al. (2018) Concept of developing a clinical decision support system for surgery of the spinal-pelvic complex. In: Methods of Computer Diagnostics in Biology and Medicine–2018. Proceedings of the All-Russian School-

Copyright© Pichkhidze Ya S, et al.

Seminar. Saratov: Amirit LLC pp: 126-128.

9. Burtsev AV, Ryabykh SO, Kotelnikov AO, Gubin AV (2017) Clinical aspects of sagittal balance in adults. Geniy Ortopedii 23(2): 228-235.

10. Byvaltsev VA, Belykh EG, Alekseeva NV, Sorokovikov VA (2013) Application of scales and questionnaires in the examination of patients with degenerative lesions of the lumbar spine: methodological recommendations. Irkutsk: FSBI NTSRVKH SB RAMS pp: 32.

11. Glazyrin DI, Rerikh VV (2009) Spondylolytic spondylolisthesis. Khirurgiya Pozvonochnika 6(1): 57-63.

12. Glantz S (1998) Biomedical Statistics. Translated from English. Moscow: Praktika pp: 459.

13. GOST R (2007) Vessels and apparatus. Norms and methods of strength calculation. General requirements.

14. Gushcha AO, Yusupov AR (2017) Evaluation of outcomes of surgical treatment of degenerative-dystrophic diseases of the spine. Khirurgiya Pozvonochnika 14(4): 85-94.

15. Dol AV, Dol ES, Ivanov DV (2018) Biomechanical modeling of variants of surgical reconstructive treatment of spinal spondylolisthesis at the L4–L5 level. Russian Journal of Biomechanics 22(1): 31-44.

16. Dol AV, Ivanov DV (2017) Development of a semi-automatic image segmentation program for creating three-dimensional models of cerebral vessels. Russian Journal of Biomechanics 21(4): 448-460.

17. Donnik AM, Ivanov DV, Kossovich L Yu, Levchenko KK, Kireev SI, et al. (2019) Creation of three-dimensional solid models of the spine with transpedicular fixation using specialized software. Izvestiya Saratovskogo Universiteta. New Series. Mathematics. Mechanics. Informatics 19(4): 424-438.

18. Dubrov VE, Zyuzin DA, Kuzkin IA, Shcherbakov IM, Donchenko SV, et al. (2019) Application of the finite element method for modeling biological systems in traumatology and orthopedics. Russian Journal of Biomechanics 23(1): 140-152.

19. Dubousset J (2016) Basic principles of vertebral surgery. Khirurgiya Pozvonochnika 4: 95-103.

20. Ivanov DV (2022) Biomechanical support of the physician's decision-making in treatment selection based on quantitative success criteria. Izvestiya Saratovskogo Universiteta. New Series. Mathematics. Mechanics. Informatics. 22(1): 62-89.

21. Ivanov DV, Barabash AP, Barabash Yu A (2015) Intramedullary rod of a new type for osteosynthesis of diaphyseal femoral fractures. Russian Journal of Biomechanics 19(1): 52-64.

22. Ivanov DV, Kirillova IV, Kossovich L Yu, Likhachev SV, Polienko AV, et al. (2021) Comparative analysis of the SpineMeter mobile application for measuring sagittal balance parameters with the Surgimap system: inter-rater reliability testing. Geniy Ortopedii. 27(1): 74-79.

23. Karlov AV, Shakhov VP (2001) External fixation systems and regulatory mechanisms of optimal biomechanics. Tomsk: STT pp: 477.

24. Clinical guidelines (2025) Degenerative spinal diseases.

25. Kobzar AI (2006) Applied Mathematical Statistics. For Engineers and Scientists. Moscow: FIZMATLIT pp: 816.

26. Kolesnikova AS, Fedonnikov AS, Kirillova IV, Ulyanov V Yu, Levchenko KK, et al. (2019) Possibilities of decision support systems in the context of surgery of the spinal-pelvic complex (analytical review). Geniy Ortopedii 25(2): 243-253.

27. Krutko AV, Baikov ES (2012) Analysis of criteria for predicting outcomes of surgical treatment of intervertebral disc herniations: a review of the current literature. Geniy Ortopedii 1: 140-145.

28. Kudyashev AL, Khominets VV, Teremshonok AV, Nagorny EB, Stadnichenko S Yu, et al. (2018) Biomechanical modeling in surgical treatment of patients with true lumbar spondylolisthesis. Khirurgiya Pozvonochnika 15(4): 87-94.

29. Mazurenko AN (2012) Transpedicular fixation of the lumbar spine in its deformities and degenerative-dystrophic lesions. Meditsinskie Novosti 4: 32-36.

30. Musatyan SA, Lomakin AV, Sartasov S Yu, Popyvanov LK, Monakhov IB, et al. (2018) Methods of medical image segmentation. Trudy Instituta Sistemnogo Programmirovaniya RAN 30(4): 183-194.

31. Müller ME, Allgöwer M, Schneider R, Willenegger H (1996) Manual of Internal Fixation: Technique Recommended by the AO Group (Switzerland). Translated from English. Moscow: Ad Marginem, pp: 750.

32. Fedonnikov AS, Kolesnikova AS, Rozhkova Yu Y, Kirillova IV, Kovtun AL, et al. (2019) Analysis of medical specialist needs in designing clinical decision support systems for traumatology and orthopedics. In: Technological

Copyright© Pichkhidze Ya S, et al.

Innovations in Traumatology, Orthopedics and Neurosurgery: Integration of Science and Practice, Saratov, 25–26 April 2019. Saratov: Amirit LLC pp: 286-288.

33. Khominets VV, Brizhan LK, Davydov DV, Khominets IV, Dol A (2019) Biomechanical rationale for using a dual-row plate with angular screw stability for treatment of patients with diaphyseal fractures of long bones. Vestnik NMHTS im. N.I. Pirogova 3(14): 60-64.

34. Zhang NZ, Xiong QS, Yao J, Liu BL, Zhang M, et al. (2022) Biomechanical changes at the adjacent segments induced by a lordotic porous interbody fusion cage. Comput Biol Med 143: 105320.

35. Kurtz SM, Devine JN (2007) PEEK biomaterials in trauma, orthopedic, and spinal implants. Biomaterials. 28(32): 4845-4869.

36. Wilcox B, Mobbs RJ, Wu AM, Phan K (2017) Systematic review of 3D printing in spinal surgery: the current state of play. Journal of Spine Surgery 3(3): 380-390.

37. Mobbs RJ, Coughlan M, Thompson R, Sutterlin CE, Phan K (2017) The utility of 3D printing for surgical planning and patient-specific implant design for complex spinal pathology: case series. Journal of Spine Surgery 3(3): 227-241.

38. Berretta S, Evans KE, Ghita O (2021) Predicting the tensile behaviour of cast acrylic resins, ULTEM 1010 and PEEK using the time-temperature superposition principle. Polymer Testing 93: 106952.

39. Han X, Yang D, Yang C, Spintzyk S, Scheideler L, Li P, et al. (2019) Carbon fiber reinforced PEEK composites based on 3D-printing technology for orthopedic and dental applications. Journal of Clinical Medicine 8(2): 240.

40. Tan XP, Tan YJ, Chow CSL, Tor SB, Yeong WY (2020) Metallic powder-bed based 3D printing of cellular scaffolds for orthopedic implants: a state-of-the-art review on manufacturing, topological design, mechanical properties and biocompatibility. Materials Science and Engineering C 108: 110410.

41. Sharma N, Aghlmandi S, Cao S, Kunz C, Honigmann P, Thieringer FM (2020) Quality characteristics and clinical relevance of in-house 3D-printed customized polyetheretherketone (PEEK) implants for craniofacial reconstruction. Journal of Clinical Medicine 9(9): 2818.

42. Zhao Y, Li B, Wang G, Ge S, Lan X, et al. (2022) Customized PEEK interbody fusion cage produced by 3D printing for cervical disc degenerative diseases: a finite element analysis. BioMed Research International 2022: 2391491.

43. Doll AV, Ivanov DV, Kirillova IV, Kossovich L Yu, Dol ES, et al. (2022) Personalized biomechanical modeling of the spine: a tool for clinical decision support in scoliosis surgery. Russian Journal of Biomechanics 26(2): 39-52.

44. Provaggi E, Capelli C, Rahmani B, Burriesci G, Kalaskar DM (2019) 3D printing assisted finite element analysis for optimising the manufacturing parameters of a lumbar fusion cage. Materials & Design 163: 107540.

Copyright© Pichkhidze Ya S, et al.

YOUR RESEARCH DESERVES GLOBAL VISIBILITY

• Publish • Discover • Share • Connect

MEDICAL	CLINICAL	LIFESCIENCES	PHARMA
90+ OPEN ACCESS JOURNALS		400+ RESEARCH TOPICS	

SUBMIT YOUR RESEARCH
Submit your manuscript through our online submission system.

REPRINTS
If you require a reprint of any article, please contact us.
info@medwinpublishers.com

BECOME A REVIEWER
Share your expertise and contribute to scholarly publishing.

SCAN TO EXPLORE MEDWIN JOURNALS

• Journals • Submit Manuscript • Reviewer Program • Article Tracking

Our Journals indexed in

Embase® ELSEVIER | PubMed National Library of Medicine NLM | Crossref | Google Scholar | INDEX COPERNICUS INTERNATIONAL | ISSN INTERNATIONAL STANDARD SERIAL NUMBER INTERNATIONAL CENTRE | ROAD DIRECTORY OF OPEN ACCESS SCHOLARLY RESOURCES | EuroPub | Scilit | WorldCat® | Academic Resource Index ResearchBib | ADVANCED SCIENCE INDEX | INTERNATIONAL Scientific Indexing | ICMJE INTERNATIONAL COMMITTEE of MEDICAL JOURNAL EDITORS

This article published by Medwin Publishers, 28475 Witherspoon Dr, Novi, MI 48377, United States, +1-248-247-6042, WhatsApp +1 (248) 275-1133, info@medwinpublishers.com

© 2026, by the Authors. The articles published from this journal are distributed to the public under "Creative Commons Attribution License" (https://creativecommons.org/licenses/by/4.0/). Therefore, upon proper citation of the original work, all the articles can be used without any restriction or can be distributed in any medium in any form.